WORKING paper

BANQUE DE FRANCE
EUROSYSTÈME

Global Sectoral Supply Shocks, Inflation, and Monetary Policy[1]

Moaz Elsayed, Christoph Grosse-Steffen, Magali Marx[2]

December 2025, WP 1026

ABSTRACT

We identify two global supply shocks that generate tensions in supply chains: shocks to transportation services and shocks to the production of highly specific intermediate inputs. Using a structural vector autoregression identified with sign, narrative, and boundary restrictions, we exploit their distinct implications for transportation costs. Transportation shocks raise shipping costs, while input production shocks lower equilibrium transportation prices by reducing output and demand for complementary services. Complementing the analysis with a global demand shock, we construct structurally interpretable, monthly indices for supply-side tensions and demand-induced congestion along global supply chains from 1969 to 2024. Both global supply shocks generate recessionary and inflationary effects in U.S. data but differ markedly in persistence and magnitude. Input production shocks produce large and persistent effects and elicit partial monetary policy accommodation, whereas transportation shocks are transitory and largely looked through.

Keywords: Supply chains, input shortages, transport shocks, structural vector autoregressions, inflation, monetary policy, demand-induced congestion.

JEL classification : C32, E31, E52, F60, R40.

[1] We would like to thank Guido Ascari, Christiane Baumeister, Fabrice Collard, Marco Del Negro, Francesco Del Prato, Valère Fourel, Domenico Giannone, Diego Känzig, Stéphane Lhuissier, Kristoffer Nimark, Lise Patureau, Gert Peersman, Franck Portier, Francesco Zanetti and seminar participants at BdF-TSE conference on Unbalanced Sectoral Inflation Dynamics, University of Helsinki, University of Bologna, Mines Paris-PSL, Toulouse School of Economics, IAAE Annual Conference 2023, EEA-ESEM Congress 2023, Society for Computational Economics Conference 2023, AFSE Annual Congress 2023, for useful discussions and suggestions.

[2] moaz.elsayed@banque-france.fr, christoph.grossesteffen@banque-france.fr, magali.marx@banque-france.fr

NON-TECHNICAL SUMMARY

Disruptions to global supply chains have become a major concern for policymakers since the Covid-19 pandemic. When deliveries are delayed or key inputs are missing, firms may slow production, lay off workers, or raise prices. Understanding how supply-chain tensions affect economic activity, employment and prices is therefore essential for the conduct of stabilization policies such as fiscal and monetary policy. This paper shows that two sources of supply-chain tensions, that are often bundled together in public debate, have distinct macroeconomic effects. The first is a transportation shock, reflecting sudden capacity losses or bottlenecks in shipping and logistics that make it harder and more expensive to move goods. The second is an input-production shock, arising from disruptions in the production of highly specific intermediate goods that firms cannot easily substitute in the short run. Both types of shocks can lengthen supplier delivery times and slow global output, but they operate through different channels.

To distinguish these shocks in the data, we use monthly global indicators of real transportation-costs, supplier delivery times, and world industrial production. The key idea is intuitive. When transportation capacity is constrained, shipping prices rise. When the production of specific inputs is disrupted, global output falls and demand for transport services declines, causing transportation prices to fall even as delivery times lengthen. We also use well-documented events – such as disasters, port closures, and maritime canal blockages – to help identify periods of severe supply chain tensions, and by bringing other information we obtain from economic theory to the empirical setup.

The estimated shocks display clear historical patterns. Transportation shocks cluster in periods of tight logistics capacity and line up with large, discrete events, such as the Suez Canal blockade in 2021 and shipping disruptions linked to the Panama Canal drought. Input-production shocks are more episodic and less clustered, with prominent spikes around major input shortage and the onset of the Covid-19 pandemic.

Both shocks are contracting economic activity and raising prices. However, their persistence differs markedly. Transportation shocks raise shipping costs and producer prices mainly in the short run and fade within two years. Input-production shocks generate larger and more persistent output losses and a longer-lasting increase in producer prices, with a gradual pass-through to consumer prices and core inflation. This reflects the difficulty of replacing missing, highly specific inputs within complex production networks.

A central contribution of the paper is the development of practical monitoring tools. We construct a Global Supply Chain Tension Index (GSTIX) that summarizes, month by month, supply chain tensions stemming from transportation and input-production shocks (Figure 1a). The index can be decomposed into these two components, allowing policymakers to identify the source of supply-chain stress. We also build a separate index capturing demand-driven congestion, labeled as Global Supply Chain Congestion Index (GSCIX), helping to distinguish supply-side tensions from strong global demand (Figure 1b).

The paper also examines how these global supply shocks affect the U.S. economy and the response of monetary policy. Both shocks reduce industrial production, raise unemployment, and affect inventories. Transportation shocks lead to a sharp but temporary rise in producer prices, with limited spillovers to consumer price inflation. Input-production shocks cause a deeper and more persistent downturn and more sustained inflationary pressures. A key finding is that the U.S. interest rates respond differently across shocks. Transportation shocks are largely looked through, while input-production shocks are followed by a clearer and more persistent tightening, consistent with their longer lasting inflationary effects. Monetary policy partly accommodates the inflation response to limit the output losses.

Figure 1.

a) Global Supply Chain Tension Index (GSTIX) b) Global Supply Chain Congestion Index (GSCIX)

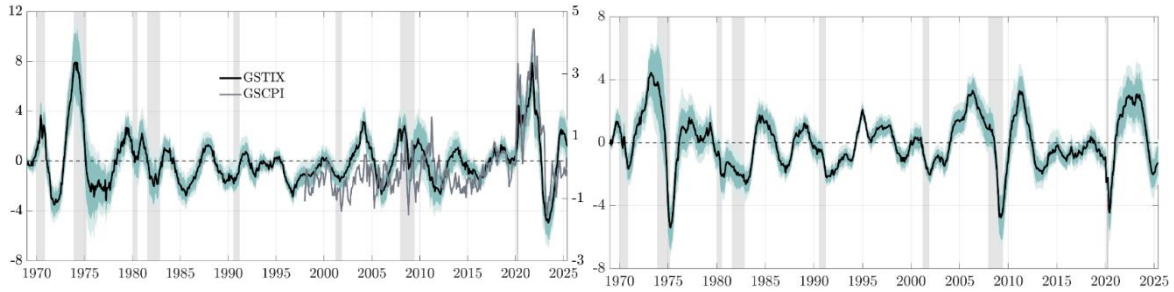

Note: Black line corresponds to the GSTIX and GSCIX, respectively, with shaded bands = 68\% and 90\% robust credible sets. Vertical grey bars denote NBER U.S. recessions. The grey line in Panel a) represents the Global Supply Chain Pressure Index (GSCPI) at rhs y-axis. ***Source:*** Authors' calculations and Applied Macroeconomics and Econometrics Center (AMEC) at the Federal Reserve Bank of New York.

Chocs d'offre sectoriels mondiaux, inflation et politique monétaire

RÉSUMÉ

Nous identifions deux chocs d'offre mondiaux qui génèrent des tensions dans les chaînes d'approvisionnement : les chocs sur les services de transport et les chocs sur la production d'intrants intermédiaires hautement spécifiques. À l'aide d'un modèle vectoriel autorégressif structurel identifié à l'aide de restrictions de signe, narratives et d'amplitude, nous exploitons leurs implications distinctes sur les coûts de transport. Les chocs sur les transports augmentent les coûts d'expédition, tandis que les chocs sur la production d'intrants font baisser les prix d'équilibre du transport en réduisant la production et la demande de services complémentaires. En ajoutant un choc de demande global, nous construisons des indices mensuels structurellement interprétables pour les tensions liées aux effets d'offre et la congestion causée par des effets de demande le long des chaînes d'approvisionnement mondiales de 1969 à 2024. Ces deux chocs génèrent des effets récessifs et inflationnistes dans les données américaines, mais diffèrent considérablement en termes de persistance et d'ampleur. Les chocs liés à la production d'intrants ont des effets importants et persistants et entraînent un assouplissement partiel de la politique monétaire, tandis que les chocs liés au transport sont transitoires et la politique monétaire « regarde donc à travers ».

Mots clés : Chaînes d'approvisionnement ; chocs sectoriels ; VAR structurel ; dynamique de l'inflation ; politique monétaire ; réseaux de production ; congestion causée par des effets de demande.

1 Introduction

Domestic production networks depend heavily on foreign inputs, often via indirect trade, making them vulnerable to international sectoral shocks. Global supply chain disruptions related to the Covid-19 pandemic led to increased interest in the topic. Causal evidence for sectoral spillovers and the estimation of input elasticities is so far based on firm-level data during natural disaster episodes and providing evidence that output effects are economically meaningful (Barrot and Sauvagnat 2016; Boehm et al. 2019; Carvalho et al. 2021). However, informing policies that are intended to stabilize production, demand and inflation requires to go beyond the analysis of case studies and to assess empirically dynamics at business cycle frequency.

We propose a structural vector autoregressive (SVAR) model to identify two global sectoral shocks that lead to tensions in global supply chains and that are often looked at jointly: (i) transportation shocks and (ii) input production shocks. Transportation shocks cause severe delays and restrictions in the flow of goods within and across countries and are due to infrastructure or operational bottlenecks. Input production shocks, in contrast, directly lead to a slowdown or impediment in manufacturing due to the shortage of upstream production inputs with high specificity, such as certain raw materials, specialized electronic parts, or any other intermediate input with high specificity.

The empirical identification is based on the combination of sign, narrative and boundary restrictions, while estimation draws on robust Bayesian inference for set-identified models following Giacomini and Kitagawa (2021); Giacomini et al. (2023). Sign restrictions are a common approach for the identification of economic shocks in SVARs, but require a consensual view about the applied signs for identification. We develop a stylized production network model to derive our assumptions for empirical identification. In this model, productivity shocks in the transportation sector and the sector for complementary intermediary input goods lead to a drop in aggregate activity as a result of downstream production effects. Supply delivery time lengthens due to imperfect substitutability between production and inventories. Key for our identification is an opposite effect of the two shocks on the equilibrium price of complementary transportation services. Transportation shocks have the conventional effect to increase transportation services prices by constraining supply. In contrast, input production shocks lower transportation prices. As less goods are being produced globally, market clearing prices for transportation services drop. The channel is lower demand for transportation services, which are complementary inputs for intermediate and final goods. Short-run rigidities in transportation supply make this price response an overall plausible assumption for the empirical model, where restrictions are only

imposed on impact. We complement the two supply-side shocks with a global demand shock.

We extend the set of identifying assumptions for supply shocks along two dimensions. First, we exploit narrative information by imposing sign restrictions on selective historical events. We focus on events which have documented effects on either production networks, as the 2011 Tōhoku earthquake in Japan, or on transportation services, for example the grounding of a container ship that led to the blockage of the Suez canal in March 2021. Second, we place weak bounds on four impact elasticities to rule out implausible short-run behavior while keeping the model set-identified. The bounds capture three facts: (i) freight demand is pro-cyclical but not infinitely elastic, so transportation costs rise only moderately with activity; (ii) higher logistics costs depress activity on impact; and (iii) more production lengthens delivery times, whereas longer delivery times do not, by themselves, bid up freight prices.

The results show that transportation and input-production shocks together account for a meaningful share of movements in world industrial production at business–cycle horizons, even though a global demand shock remains the dominant driver of output volatility. Regarding transportation, the two sectoral shocks explain most of the variation in real transportation costs at all horizons, while their contribution to supplier delivery times is large and front-loaded, gradually giving way to global demand as bottlenecks clear. Based on those results, we construct a Global Supply Chain Tension Index (GSTIX) by aggregating the contributions of the two sectoral supply shocks in the historical decomposition of supplier delivery time and transportation cost from 1968 to 2024 at monthly frequency. The index has a structural interpretation and can be decomposed into a transportation and an input-production component. We also build a Global Supply Chain Congestion Index (GSCIX) that sums the contribution of a global demand shock to the same two variables and tracks demand-driven tightness leading to longer delivery times and higher shipping costs. The GSTIX co-moves strongly with bottom-up measures of global supply-chain pressure (Benigno et al., 2022), while the GSCIX closely tracks demand rebounds.

Next, we study transmission in a block-exogenous setting for the United States and global commodities. A main result is that both sectoral shocks are contractionary and inflationary, hence lead to the responses traditionally associated with supply shocks. The strength, timing, and persistence of the price response differ across the two shocks. A transportation shock lowers U.S. industrial production, raises producer prices with a clear hump, and generates only modest, short-lived increases in PCE and core PCE, whereas an input-production shock produces a deeper and more persistent contraction together with a more durable rise in producer prices and a more sustained, though

still moderate, pass-through to consumer prices. Real activity declines, unemployment rises, and inventories adjust in both regions, in line with capacity constraints and sequencing frictions along supply chains. These empirical patterns are consistent with real-side amplification through input–output linkages in industries that rely on foreign inputs (Acemoglu et al., 2012; Baqaee, 2018; Dhyne et al., 2021). The significant price responses can be rationalized with sectoral price stickiness (Afrouzi and Saroj, 2023), and with trade-cost pass-through that amplifies the propagation of transportation cost shocks to free-on-board prices (Hummels and Skiba, 2004; Daudin et al., 2022).

The long sample period allows us to study the systematic response of monetary policy to the two supply disturbances. Importantly, we find that U.S. monetary policy reacts differently to the -side shocks. Transportation shocks are largely "looked through," with the one-year interest rate showing little systematic tightening despite higher producer prices and temporary consumer-price increases. In contrast, input-production shocks are followed by a clear and sustained rise in the one-year interest rate, in line with persistent inflation and a deeper production downturn generated by this shock. Since interest rates move by less than inflation, the monetary policy partly accommodates the inflation response to preserve production.

Turning to global commodities, both shocks are inflationary for oil and broad commodity prices. Transportation shocks generate a hump-shaped build-up in the real price of oil and in the commodity index that fade only after two years. Input-production shocks deliver even more persistent increases in oil and commodities prices. These commodity-price patterns reinforce the pricing pressure seen in producer prices and help account for the persistence differences across the two shocks.

We find that post-pandemic inflation is consistent with the channels identified in our parsimounious SVAR. In 2022, both transportation and input-production shocks contributed to the surge in U.S. PCE and core PCE inflation, with input-production shocks accounting for most of the increase in producer prices. As congestion eased in 2023, transportation shocks became disinflationary, while input-production shocks continued to push U.S. consumer and producer prices upwards. By 2024, the contributions of both sectoral shocks to consumer inflation were small and often not statistically distinguishable from zero, with some remaining sectoral-supply influences concentrated in upstream producer prices.

Our work is related to mainly two sets of papers. Quantifying the role of sectoral shocks for business cycle dynamics is a classic question studied in a number of works since Long and Plosser (1983, 1987). Horvath (2000) proposes a model where all aggregate fluctuations are driven by independent sectoral shocks. More recent contributions focus on the amplification arising from sectoral shocks in complex networks (Acemoglu

et al., 2012; Baqaee, 2018; Dew-Becker, 2023; Afrouzi and Saroj, 2023). Our paper contributes to this theoretical literature by showing empirically that significant real effects originate from input production shocks and transportation shocks in the US data. We consider sectoral supply shocks as being of global relevance, motivated by the observation that production networks depend on foreign inputs (Dhyne et al., 2021). Our paper also draws on results from this literature for the identifying assumptions, which is based on a differentiated price responses in the transportation services sector through demand complementarities. We consider this mechanism to be distinct from supply shocks causing deflation via negative income effects that have been put forward as Keynesian supply shocks in the literature (Guerrieri et al., 2022).

Our paper relates to a growing number of empirical papers that study the propagation of localized shocks through production networks. Boehm et al. (2019) document Boehm et al. (2019) firm-level spillovers from the 2011 Tōhoku earthquake in Japan. They find a short-run elasticity of substitution between different inputs of near zero, suggesting large adjustment frictions and output losses in response to shocks in the production network leading to input shortages. Barrot and Sauvagnat (2016) estimate the network effects of natural disasters in U.S. firm-level data in a sample covering 30 years. They find that customers of firms affected by natural disasters suffer substantial output losses.

More closely related to our approach are recent contributions in a time-series setup. Burriel et al. (2024) develop a newspaper based index of supply bottlenecks for six advanced economies. They assess the macro effects of exogenous changes in their index based on a Cholesky identification approach, finding that they dampen industrial production and employment, and increase CPI inflation. Bai et al. 2024 estimate the effects of supply chain disruptions by mobilizing satellite data for 50 ports to construct a measure of port congestion over the period 2017-01 to 2022-04. Känzig and Raghavan (2025) also focus on disruptions in the transportation sector by exploiting high frequency surprises in shipping rates at short windows around events related to disruptions at the Suez and Panama canal, respectively, with a stagflationary effect on the U.S. economy. Focusing on shortages of input goods, Caldara et al. (2025) construct a newspaper article based monthly shortages index. They find that shortages help improve inflation forecasts, but exogenous increases in shortages have limited effects on U.S. consumer prices in a VAR-based analysis. Our paper departs from these approaches by considering a setup for joint identification of transportation shocks and input production shocks and by studying their differentiated effect on the U.S. economy.

The remainder of the paper is organized as follows. Section 2 presents the empirical

model, data and identifying assumptions for robust Bayesian inference for set-identified models. Section 3 reports the baseline results, including the construction of the indices capturing tensions in global supply chains and demand congestion. Section 4 presents the macroeconomic effects for the U.S. economy and commodity prices. Section 5 concludes.

2 Empirical model and identification

This section sets up the empirical model. It presents three sets of identifying assumptions made in the baseline model, namely sign-restrictions, shock-sign restrictions from narrative episodes, and prior information on elasticities from economic theory. The section also discusses the robust Bayesian estimation approach with multiple priors used for the set-identified model (Giacomini et al., 2023).

2.1 Model setup and data

The empirical model takes the form of a structural vector autoregression (SVAR). Let $\boldsymbol{y}_t$ be an $n \times 1$ vector of variables following the SVAR(p) process

$$\boldsymbol{A}_0 \boldsymbol{y}_t = \boldsymbol{A}_+ \boldsymbol{x}_t + \boldsymbol{\epsilon}_t, \quad t = 1, ..., T \tag{1}$$

where the vector $\boldsymbol{x}_t = (\boldsymbol{y}'_{t-1}, ..., \boldsymbol{y}'_{t-\ell}, ..., \boldsymbol{y}'_{t-p}, \boldsymbol{c}, t)$ contains lagged endogenous variables up to lag $\ell = p$, a vector of constants $\boldsymbol{c}$, and a linear trend, $\boldsymbol{A}_+ = (\boldsymbol{A}_1, ..., \boldsymbol{A}_\ell, ..., \boldsymbol{A}_p, \boldsymbol{A}_c)$, and structural shocks $\boldsymbol{\epsilon}_t \overset{\text{iid}}{\sim} \mathcal{N}(0_{n\times 1}, \boldsymbol{I}_n)$. Let $m = \dim(\boldsymbol{x}_t)$ denote the number of regressors. The reduced form of the model can be expressed as

$$\boldsymbol{y}_t = \boldsymbol{B} \boldsymbol{x}_t + \boldsymbol{u}_t, \quad t = 1, ..., T \tag{2}$$

where $\boldsymbol{B} = (\boldsymbol{B}_1, ..., \boldsymbol{B}_p, \boldsymbol{B}_c)$, with $\boldsymbol{B}_\ell = \boldsymbol{A}_0^{-1} \boldsymbol{A}_\ell$ and $\boldsymbol{u}_t = \boldsymbol{A}_0^{-1} \boldsymbol{\epsilon}_t$, with the reduced form errors $\boldsymbol{u}_t \overset{\text{iid}}{\sim} \mathcal{N}(0_{n\times 1}, \boldsymbol{\Sigma})$. The covariance matrix of the reduced-form residuals is given by

$$E(\boldsymbol{u}_t \boldsymbol{u}'_t) = \boldsymbol{\Sigma} = \boldsymbol{A}_0^{-1} (\boldsymbol{A}_0^{-1})'. \tag{3}$$

Let $\boldsymbol{\phi}$ denote the set of reduced form parameters such that $\boldsymbol{B}, \boldsymbol{\Sigma} \in \boldsymbol{\phi}$, while structural parameters are denoted by $\boldsymbol{\theta}$, such that $\boldsymbol{A}_0, \boldsymbol{A}_+ \in \boldsymbol{\theta}$.

Data. We set $\boldsymbol{y}_t = (s_t, z_t, y_t)'$ to be a vector containing a measure of transportation cost (s_t), supply delivery time (z_t), and world industrial production (y_t). Throughout, s_t is in logs, z_t is in levels, and y_t is in first difference of the log. Transportation costs are expressed in real cost from a large cross-section of shipping and air freight

indices, extending a measure proposed by Kilian (2009). See Online Appendix B.2 for details on the construction of the index. Supplier delivery time is a monthly index compiled by the Institute of Supply Management from a survey among firm managers. It tracks changes in the speed of supplier delivery time. Values above 50 indicate slower delivery speed, while faster delivery speed is associated with values below 50. The information contained in the data is used by practitioners to decide when to place orders to prevent running out of inventories. Finally, global industrial production corresponds to the monthly industrial production of OECD countries plus six major emerging market economies, following Baumeister and Hamilton (2019). All data sources are described in the Online Appendix B.1. In the baseline analysis, we use monthly data from January 1968 to June 2025. The starting period is given by the availability of transportation cost series.

The model equations for transportation cost, supplier delivery time, and world industrial production from the structural model (1) are:

$$s_t = \alpha_{sz} z_t + \alpha_{sy} y_t + \boldsymbol{a}_{1+}' \boldsymbol{x}_t + \epsilon_{1t}, \tag{4}$$

$$z_t = \alpha_{zs} s_t + \alpha_{zy} y_t + \boldsymbol{a}_{2+}' \boldsymbol{x}_t + \epsilon_{2t}, \tag{5}$$

$$y_t = \alpha_{ys} s_t + \alpha_{yz} z_t + \boldsymbol{a}_{3+}' \boldsymbol{x}_t + \epsilon_{3t}, \tag{6}$$

where $\boldsymbol{a}_{i+}'$ denotes the ith row of $\boldsymbol{A}_+$ for $i = 1, 2, 3$, and $\boldsymbol{\epsilon}_t = (\epsilon_{1t}, \epsilon_{2t}, \epsilon_{3t})'$.

Equation (4) represents the market for transportation services. Transportation costs s_t are determined contemporaneously by supplier delivery time, via the coefficient α_{sz} capturing bottlenecks in global supply chains, by global demand conditions through α_{sy}, and by a structural transportation supply shock ϵ_{1t}. Equation (5) summarizes the determinants of supplier delivery time z_t: one ingredient is transportation services, as implied by α_{zs}, another is global demand through α_{zy}, while other factors that slow down delivery are captured by the structural input production shock ϵ_{2t}. Finally, global activity y_t enters the model through equation (6) and depends on transportation costs (α_{ys}), supplier delivery time capturing the availability of intermediate inputs (α_{yz}), and a structural global demand shock ϵ_{3t}. We set the lag length to $p = 12$, so that the regressor vector $\boldsymbol{x}_t$ includes twelve lags of all variables, a constant, and a linear time trend, $\boldsymbol{x}_t = (\boldsymbol{y}_{t-1}', \ldots, \boldsymbol{y}_{t-12}', 1, t)'$.

The corresponding matrix $\boldsymbol{A}_0$ is given by

$$\boldsymbol{A}_0 = \begin{pmatrix} 1 & -\alpha_{sz} & -\alpha_{sy} \\ -\alpha_{zs} & 1 & -\alpha_{zy} \\ -\alpha_{ys} & -\alpha_{yz} & 1 \end{pmatrix}. \tag{7}$$

2.2 Identification and robust Bayesian inference

This section motivates our choice of robust Bayesian inference over estimation methods applying conjugate priors. To clarify the interaction of the three sets of identifying assumptions put forward below, it will be useful to restate model (2) in its orthogonal-reduced form, as it is common for set-identified SVARs:

$$\boldsymbol{y}_t = \boldsymbol{B}\boldsymbol{x}_t + \boldsymbol{P}\boldsymbol{\eta}_t, \quad t = 1, ..., T \tag{8}$$

where $\boldsymbol{P}$ denotes the lower-triangular Cholesky factor of $\boldsymbol{\Sigma}$, thus $\boldsymbol{\Sigma} = \boldsymbol{P}\boldsymbol{P}'$, and we have normalized the variance-covariance matrix $E(\boldsymbol{\eta}_t\boldsymbol{\eta}_t') = \boldsymbol{I}_n$, with reduced-form VAR innovations $\boldsymbol{u}_t = \boldsymbol{P}\boldsymbol{\eta}_t$. Candidate solutions for structural shocks can then be obtained from

$$\boldsymbol{\epsilon}_t^* = \boldsymbol{Q}'\boldsymbol{\eta}_t, \tag{9}$$

where $\boldsymbol{Q}'$ is a $n \times n$ square orthogonal matrix such that $\boldsymbol{u}_t = \boldsymbol{P}\boldsymbol{\eta}_t = \boldsymbol{P}\boldsymbol{Q}\boldsymbol{\epsilon}_t^*$ (Kilian and Lütkepohl, 2017). Note that any candidate matrix $\boldsymbol{Q}$ is a draw from the set of all orthogonal matrices fulfilling the condition $\mathcal{O}(n) = \{\boldsymbol{Q} \mid \boldsymbol{Q}\boldsymbol{Q}' = \boldsymbol{I}_n\}$.

Our approach to identification of three structural shocks in (2) falls short of fulfilling the sufficient number of zero restrictions for point-identification, leaving us with the task of estimating a set-identified system (Rubio-Ramírez et al., 2010). Available algorithms for Bayesian estimation of set-identified SVARs, such as Arias et al. (2018), propose a conjugate prior to generate independent draws over structural parameterization. Such a prior can be decomposed into a prior for the reduced-form parameter, which is revised by the data, and the prior for the structural parameter given the reduced-form parameters, which is not revised by the data (Giacomini and Kitagawa, 2021). The latter implies a uniform distribution over $\mathcal{O}(n)$. While the implicit prior is assumed to be uninformative on the rotation of the $\boldsymbol{Q}$ matrix itself, Baumeister and Hamilton (2015) have shown that it may well be informative for other parameters of the model.

We impose three sets of identifying assumptions on structural parameters $\boldsymbol{\theta}$, or functions thereof, in order to give economic interpretation to the orthogonalized shocks $\boldsymbol{\epsilon}_t^*$ in equation (9). First, we use sign restrictions (SR) on the structural parameters via restrictions on elements of $(\boldsymbol{A}_0^{-1})'$. Specifically, this limits the contemporaneous response of the ith variable to the jth shock. Second, we impose boundary restrictions (BR) that limit the magnitude of the contemporaneous response of the ith variable to the jth shock (Kilian and Murphy, 2012). Third, shock-sign restrictions from narrative events (NR) are imposed, which require that a structural shock ϵ_{1k} for some $k \in \{1, ..., T\}$ is either positive or negative, according to the narrative event. This last

set of restrictions introduces a direct dependence of the set-valued mapping from $\boldsymbol{\phi}$ to $\boldsymbol{\theta}$ on the realization of the data.

We estimate the model using a robust Bayesian approach suggested by Giacomini and Kitagawa (2021) *(henceforth GK21)* that eliminates prior sensitivity, and which was extended by Giacomini et al. (2023) *(henceforth GKR23)* to account for narrative restrictions. Intuitively, the procedure explores the sensitivity of any object of interest, e.g. the IRF, to the choice of the prior for the flat part of the likelihood that is not revised by the data. Formally, we follow the notation in GKR23 and let $\mathscr{Q}(\boldsymbol{\phi} \mid SR, BR, NR, \boldsymbol{Y}^T)$ denote the set of observationally equivalent parameter points, such that it is possible to denote the set of all conditional priors for $\boldsymbol{Q}$ that are consistent with the identifying restrictions as $\Pi_{\boldsymbol{Q}|\boldsymbol{\phi}} = \big\{\pi_{\boldsymbol{Q}|\boldsymbol{\phi}} : \pi_{\boldsymbol{Q}|\boldsymbol{\phi}}\big(\mathscr{Q}(\boldsymbol{\phi} \mid SR, BR, NR, \boldsymbol{Y}^T)\big) = 1\big\}$, where $\boldsymbol{Y}^T = (\boldsymbol{y}_1, ..., \boldsymbol{y}_T)$. In our application, we seek obtaining a robust set of a scalar value $\eta \in \mathcal{H}$ (or functions thereof), representing for example an impulse response function $\eta = h(\boldsymbol{\theta})$. The robust procedure applies Bayes rule to each (conditional) prior $\Pi_{\boldsymbol{Q}|\boldsymbol{\phi}}$, and computes the point-wise posterior lower (and upper) probability that satisfy the restrictions, denoted by $\pi_{\eta|Y*}(\cdot)$ and $\pi^*_{\eta|Y}(\cdot)$, respectively, and represent the infimum and supremum probabilities for the object of interest based on the researchers joint set of identifying assumptions. Intuitively, this amounts to minimizing the posterior probability for $\boldsymbol{\phi}$ to fall within $\mathscr{Q}(\cdot)$. This can be interpreted, in the words of GK21, as saying that 'the posterior credibility for $\eta \in \mathscr{Q}(\cdot)$ is at least equal to $\pi_{\eta|Y*}(\cdot)$, no matter which unrevisable prior one assumes'.

GKR23 demonstrate how to extend this procedure to the case of narrative restrictions, where a difficulty arises from the data-dependent mapping from $\boldsymbol{\phi}$ to $\boldsymbol{Q}$. By considering for the posterior only values of $\boldsymbol{Q}$ that are consistent with sign restrictions and narrative restrictions, the NR effectively truncate the prior for $\boldsymbol{Q} \mid \boldsymbol{\phi}$. Then, using every possible prior in the set of conditional priors allows computing the set of posteriors for $(\boldsymbol{\phi}, \boldsymbol{Q})$, which is now not only conditional on the validity of all traditional restrictions ($D_N = 1$), but also on the data $\boldsymbol{Y}^T$. We denote this set of posteriors as $\Pi_{\boldsymbol{\phi},\boldsymbol{Q}|\boldsymbol{Y}^T, D_N=1}$, from which it is possible to obtain the set of posteriors for η, denoted by $\Pi_{\eta|\boldsymbol{Y}^T, D_N=1}$ through $\eta = h(\boldsymbol{\theta}(\boldsymbol{\phi}, \boldsymbol{Q}))$. It is in the sense of data-conditionality that the suggested approach arrives at a 'conditional identified set'.

Ultimately, we compute a robust credible region C^*_α with credibility level $\alpha \in (0, 1)$ for η directly from the posterior distribution of $\boldsymbol{\phi}$ by minimizing a volume-distance criterion. Specifically, GK21 consider a subset $C_\alpha \subset \mathcal{H}$ such that

$$\pi_{\eta|Y*}(C_\alpha) = \pi_{\boldsymbol{\phi}|Y}\left(\boldsymbol{\phi} : \mathrm{IS}_\eta(\boldsymbol{\phi} \mid SR, BR, NR, \boldsymbol{Y}^T) \subset C_\alpha\right) \geq \alpha, \tag{10}$$

where $\mathrm{IS}_\eta(\cdot)$ is the identified set of impulse response functions derived from observa-

tionally equivalent values of $\boldsymbol{Q}$. Recall that the likelihood within $\text{IS}_\eta(\cdot)$ is flat, leading to multiplicity for C_α. GK21 suggest pinning down a unique value C_α^* by minimizing the point-wise volume of a distribution of distance measures $d(\eta_c, \text{IS}_\eta(\boldsymbol{\phi}))$ at the αth quantile of this distribution, where η_c denotes a candidate IRF from the identified set $\text{IS}_\eta(\cdot)$. Ultimately, one can refer to C_α^* as the *smallest robust credible region with credibility* α. In all figures we report 68% and 90% smallest robust credible regions.

The model is estimated from the conjugate diffuse reduced-form posterior implied by a flat prior on B and a Jeffreys prior on Σ, truncated to the set of stable VARs. Equivalently, we draw $\Sigma \sim \text{IW}(S, T-m)$ and $\text{vec}(B) \mid \Sigma \sim \mathcal{N}(\text{vec}(\hat{B}), \Sigma \otimes (X'X)^{-1})$, discarding unstable draws, where $X = (\boldsymbol{x}_1, ..., \boldsymbol{x}_T)'$ is the $T \times m$ matrix of regressors, $\hat{B}$ is the OLS estimate of B, and S is the associated sum-of-squares matrix. For the baseline specification, we obtain 1,000 draws that satisfy all restrictions (sign, boundary, and narrative) simultaneously.

In the following sections, we explain in detail all identifying assumptions we impose for identification.

Sign Restriction 1: [**transportation shock**] *A transportation shock lowers global industrial production and increases supplier delivery time and transportation cost.*

Second, a negative input production supply shock (henceforth *input production shock*) refers to any disruptions in the production of goods, excluding oil, that lead to decreased supply of intermediate or final goods. This type of shock can occur due to various reasons such as natural disasters, labor strikes, power outages, equipment failure leading to business interruptions, and other factors that affect the smooth operation of production lines. For example, a factory fire could cause an input production shock for a specialized product, impeding downstream production due to a high specificity of the missing good. Another example is a labor strike that shuts down a production line, resulting in a temporary halt in production and potentially causing a shortage of goods. Finally, any export restrictions of supplies of critical material would also fall within this category. Input production shocks can cause adverse economic consequences that are not limited to downstream sectors due to production complementarities (Acemoglu et al., 2012). Importantly for identification, we think of transportation services as a complementary good, which will be in lower demand if negative input production shock dampens output. This induces ceteris paribus the market clearing price for transportation services to drop, which is reinforced through the rigid supply of transportation services due to installed capacity, for example a fixed number of container ships in the short run.

Sign Restriction 2: [**input production shock**] *An input production shock lowers global industrial production, raises supplier delivery time, and lowers transportation*

cost.

Third, a global demand shock captures broad demand-driven movements in output that raises contemporaneous utilization of logistics capacity, driving up supplier delivery time and transportation cost.

Sign Restriction 3: [**global demand shock**] *A global demand shock increases global industrial production, transportation cost, and supplier delivery time.*

Micro-foundations. The three sign patterns are micro-founded by a simple production-network model developed in Online Appendix A. Short-run rigidity in transportation supply and complementarity between transportation services and upstream inputs imply: (i) transportation bottlenecks raise freight prices and lengthen delivery times; (ii) input-production shortfalls lower freight prices while still lengthening delivery times; and (iii) stronger activity raises the demand for freight and, hence, transportation costs. These implications map one-for-one into the sign restrictions used below.

Combining restrictions 1–3, we impose sign restrictions on A_0^{-1} (rows ordered as s = transportation cost, z = supplier delivery time, y = global industrial production; columns ordered as transportation, input production, and global demand shocks) such that

$$\text{sign}(A_0^{-1}) = \begin{pmatrix} + & - & + \\ + & + & + \\ - & - & + \end{pmatrix}. \tag{11}$$

These sign restrictions imply $\alpha_{yz} < 0$, $\alpha_{zs} > 0$, and $\alpha_{sy} > 0$.

2.3 Boundary constraints

We use additional prior information from the existing literature in order to reduce the number of eligible empirical models further. While this approach has been introduced by Kilian and Murphy (2012) in the context of a model using an uninformative prior on the rotation matrix, we argue that this type of restriction is particularly useful for the context of robust Bayesian estimation with multiple priors. In essence, the approach imposes assumptions on structural parameters on the contemporaneous effects summarized in Tab. 1.

Assumption BR1 implies a transportation cost elasticity to supplier delivery time below zero. We infer this restriction from the work of Alessandria et al. (2023), who model the effects of shipping delays for the US economy over the pandemic. They find that a shipment delay lowers imports, production and consumption. While they

Table 1: Assumptions regarding boundary restrictions

#	struct. param.	description	interval
(BR1)	α_{sz}	transp. cost elast. to supply deliv. time	$[-\infty, 0]$
(BR2)	α_{ys}	output elast. to transportation cost	$[-\infty, 0]$
(BR3)	α_{sy}	income elasticity of demand for transp.	$[0, 2]$
(BR4)	α_{zy}	supply deliv. time elast. to production	$[0, 3]$

do not have variable transportation cost in their model, we infer from the aggregate responses that transportation services real costs should drop.

Assumption BR2 builds on the central idea quite present in the literature that lower transportation cost stimulate economic activity. Transportation cost can drop for example due to higher productivity and innovation, which Coşar et al. (2024) associate with long-run increases in GDP. (Hummels et al., 2009) associate increased competition in the transportation sector with lower transportation cost and higher trade and imports. Kilian et al. (2023) summarize unexplained variation in transportation cost as frictions in container shipping, which also negatively correlate with US industrial production and household consumption in their findings.

Assumption BR3 is informed directly by estimates from the literature. Kilian et al. (2023) find that foreign and domestic demand shocks raise transportation cost, but by less than one for one, suggesting a value between zero and one. Tjandra et al. (2024) document that the income elasticities for transportation demand for a broad range of transportation freight services (rail, road, marine, and aviation) and across various country clusters is positive and estimated between 1.5–2. The range is also supported by Oum et al. (1990), who find relatively low price elasticity of demand for freight transport ranging from 0 to 2. Hence, we limit the interval of plausible estimates to this range.

Assumption BR4 postulates that higher output raises supplier delivery time. While standard macroeconomic models do not consider load-dependent production time of goods, the relationship between quantities (e.g. number of customers) and waiting time is well-known as "Little's law" (Little, 1961) from queuing systems. The operations research literature defines lead time as the duration between placing an order and receiving the final product. It is a performance indicator in supply chains. Studies that quantify the relationship between the production load and lead time at the firm level find that these feature a hockey stick relationship. While increases in production load initially do not raise lead time, rapid increases in lead time can accrue when certain thresholds are exceeded and further orders are placed (Cannella et al., 2018). The slope of this upward reaching path is determined by the responsiveness of the

company, which is given by a wide range of factors such as the way raw materials are sourced or the efficiency of inventory management. Translating these considerations to aggregate relationship between global industrial production and supply delivery time is non-trivial. At the aggregate level, the non-linearities should be smoothed out via substitution between goods and suppliers, why we assume an upper bound of $\alpha_{zy} \in [0, 3]$.

Our impact sign restrictions on the columns of $(\boldsymbol{A}_0^{-1})'$ imply three contemporaneous cross-elasticities in $\boldsymbol{A}_0$ with known signs: $\alpha_{yz} < 0$, $\alpha_{sy} > 0$, and $\alpha_{zs} > 0$. Economically, $\alpha_{yz} < 0$ captures that longer supplier delivery times (congestion/delays) depress contemporaneous activity by slowing the arrival of intermediary goods; $\alpha_{sy} > 0$ reflects that stronger activity raises the demand for freight services, putting upward pressure on transportation cost; and $\alpha_{zs} > 0$ is consistent with higher transportation cost signaling capacity strain that lengthens supplier delivery times.

2.4 Narrative restrictions

We refine identification by imposing one-month impact sign restrictions on the structural shocks in months associated with plausibly exogenous disruptions to transportation or input production. Tab. 2 lists the episodes and dates used as restrictions.

Table 2: Episodes used for narrative sign restrictions (on-impact, one month)

Event	**Date**
Transportation shocks	
Great Hanshin (Kobe) earthquake	January 1995
Hurricane Katrina	September 2005
Eyjafjallajökull eruption	April 2010
Hanjin Shipping bankruptcy	September 2016
Suez Canal grounding	March 2021
Panama Canal drought	August 2023
Red Sea attacks	November 2023
Input-production shocks	
Benguela railway closure (cobalt)	August 1975
Shaba invasion / cobalt crisis	May 1978
Chi-Chi (Taiwan) earthquake	September 1999
Sichuan (Wenchuan) earthquake	May 2008
Tōhoku earthquake and tsunami	March 2011
Thailand floods	October 2011

Transportation-shock episodes

- January 1995 is considered as transportation disruption due to the Great Hanshin–Awaji (Kobe) earthquake on 17 January 1995. At the time the 6th largest container terminal in Japan and the connection to Japans second largest economic region, quay-wall failures from soil liquefaction, toppled cranes, and widespread berth damage led to 90 percent destruction and its quasi shutdown for two years (Chang, 2000). This had devastating economic consequences in the Hyōgo prefecture (Hiroshi and Hsiao, 2015).

- September 2005 corresponds to Hurricane Katrina, which lead to destruction and closure of Gulf coast ports and navigation channels in the Lower Mississippi River, an important gateway for varios bulk materials (Frittelli, 2005). Friedt (2021) finds sizable and persistent trade reductions from US port-level data, which are partly offset by rerouting to neighboring ports (Sytsma, 2020).

- April 2010 marks the eruption of Iceland's Eyjafjallajökull vulcano. In its aftermath the volcanic ash plume forced largeareas of European airspace to close for a week, cancelling more than 100,000 flights (Budd et al., 2010). Air freight volume dropped by around 5-6 percent, affecting temporarily trade between the US and Europe (Besedeša and Murshid, 2018).

- September 2016 captures the bankruptcy of Hanjin Shipping, the 7th largest container carrier in the world, which stranded vessels and boxes and created short-run port congestion. The Korean company was linked to various container terminal assets which led to further service gaps (Kwon, 2021).

- March 2021 refers to the grounding of the container ship 'Ever Given' in the Suez Canal (23–29 March), which halted transits for six days and delayed onward port calls (Suez Canal Authority, 2021). 25 container ships heading to ports at the US east coast got delayed with a sizeable trade volume of 217,400 TEUs (Bureau of Transportation Statistics, 2021).

- August 2023 denotes a Panama Canal incident in response to a prolonged drought, as water levels in Gatún Lake dropped to an extend that locks could no longer be operated at usual frequency. The port authority limited daily transits and required ships to lighten their load. As a consequence, Chico et al. (2024) identified more than 290 vessels that were forced to take alternative transit routes, usually longer, leading to higher transportation cost and shipping delays, notably at US ports.

- November 2023 marks the onset of attacks by Houthi forces on commercial vessels. The OECD's International Transportation Forum reports that between 1 November 2023 and 28 February 2024, the number of ships transiting the Bab-el-Mandeb Strait decreased by 55 percent. Rerouting via the Horn of Africa can take from 8 to 17 additional days, depending on the vessel type, leading to shipping delays that initially perturbed supply chains, while rerouting was subsequently integrated in plans for inventory orders (ITF, 2024).

Input-production-shock episodes

- August 1975 corresponds to the Angolan civil-war closure of the Benguela Railway linking the mineral rich region of Katanga in Democratic Republic of Congo (DRC) to the port of Lobito, running through the hinterland of Angola. Price speculation and delayed supply and supply constraints had implications for industries that had to adapt quickly (Habib et al., 2016; Gulley, 2022).

- May 1978 (Shaba II) marks renewed conflict in the Shaba region in southern Zaire, today DRC, that further affected mining and processing operations (Habib et al., 2016).

- September 1999 captures the Chi-Chi (Taiwan) earthquake with a magnitude of 7.6, where widespread power outages and facility damage produced short-lived but sharp interruptions in electronics and semiconductor output (Noy and duPont, 2016).

- May 2008 denotes the Wenchuan earthquake in the Sichuan Province of China, which generated substantial industrial losses—especially in chemicals—with upstream bottlenecks propagating via input linkages to distant regions in China (Huang et al., 2022).

- March 2011 is the Tōhoku earthquake in Japan, which caused supply-chain disruptions that propagated to downstream manufacturers abroad through imported inputs. Boehm et al. (2019) document significant spillovers to US manufacturing production via elevated production elasticities at the firm level.

- October 2011 refers to the Thailand floods, where increased rainfall in the early monsoon season related to La Niña event caused damage along the Chao Phraya River which, as it approaches Bangkok, concentrates two thirds of national GDP (UNISDR, 2012). The disaster affected manufacturing in automotive and electronics parts (Haraguchi and Lall, 2015), propagating via supply chains to foreign buyers as far as Sweden. Forslid and Sanctuary (2023) find that output of Swedish firms exposed to Thai exporters dropped in 2012 by 8 percent.

Figure 1: Posterior distributions of contemporaneous elasticities

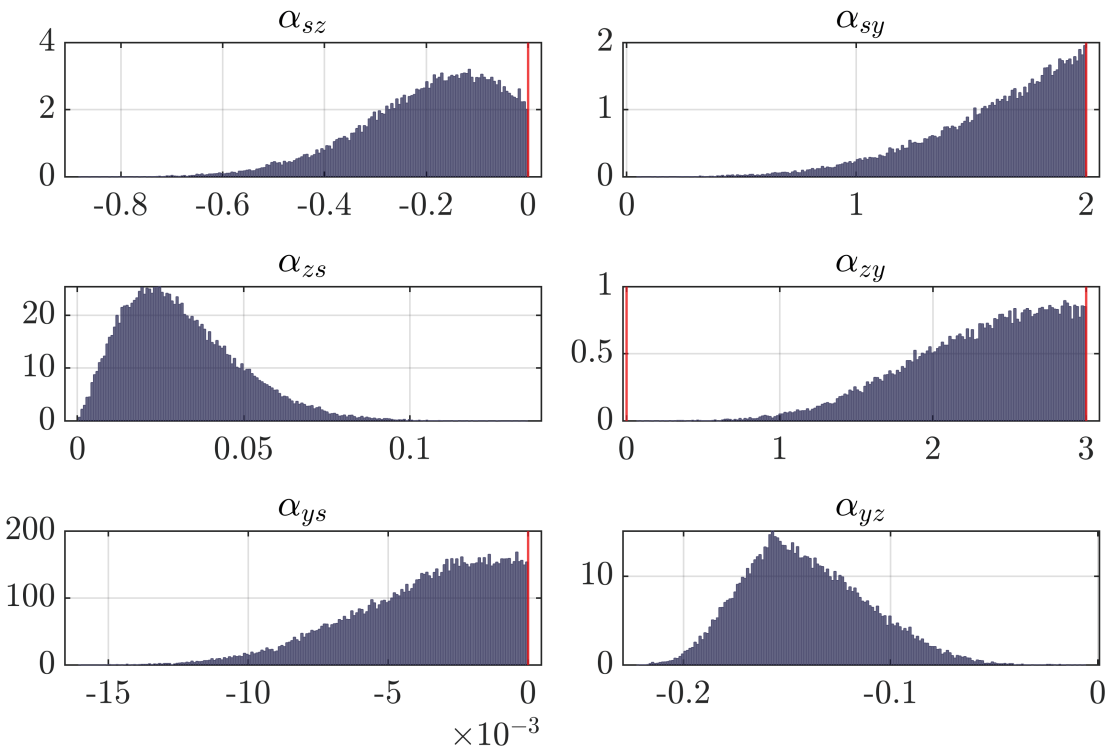

Notes: Histograms show posterior draws of the six contemporaneous elasticities under the baseline identification that combines sign restrictions with narrative and boundary restrictions. Vertical red lines mark BR bounds where applicable.

Fig. 1 reports the posterior distributions of the six contemporaneous elasticities under the baseline identification that jointly imposes sign, narrative, and boundary restrictions. The posteriors are tight and economically plausible, and each layer of identifying assumptions provides valuable information contributing to model selection.[1]

3 Estimation results

This section presents the results based on the three variable structural VAR. In addition to more standard results on the dynamics, we compute novel measures of supply chain disruptions based on the structurally identified model.

[1]Online Appendix C discusses elasticity posterior densities for the set of models identified by i) SR only, ii) combining SR and BR, as well as iii) combining SR and NR. Each set of identifying assumptions leads to posterior distributions that are less spread out, hence contributing to the model selection by sharpening identification.

3.1 Evolution of global sectoral supply shocks

Fig. 2 shows the time series of global sectoral supply shocks from our SVAR at monthly frequency. The top panel is the transportation supply shock and the bottom panel is the input-production supply shock.

The transportation shock is mostly positive in 2021–2022, consistent with tight logistics capacity and congestion. The input-production shock spikes at historicaly high values in early 2020, before turning negative after reopening after the first lockdown. We also see a short dip in the input-production shock around April 2022 (China lockdowns) and renewed transportation disturbances in late 2023–2024 when shipping routes were rerouted due to the Panama canal drought and Red Sea crisis.

Figure 2: Historical evolution of supply shocks

(a) Transportation supply shock

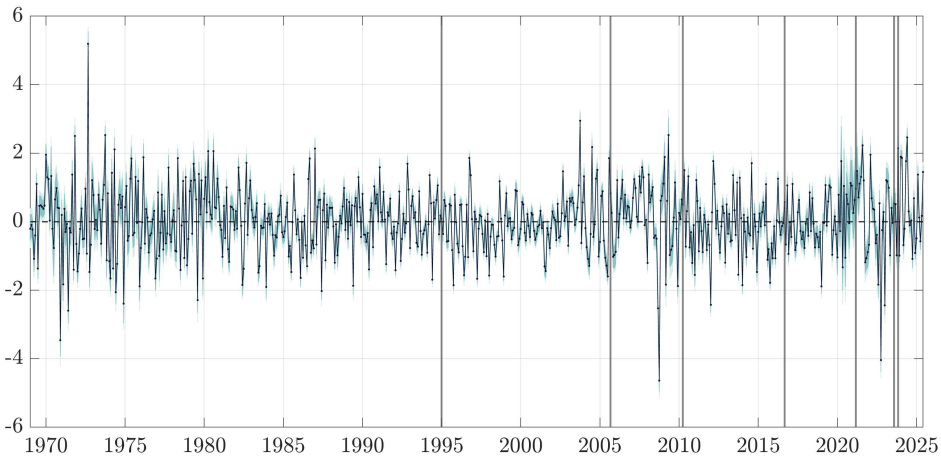

(b) Input-production supply shock

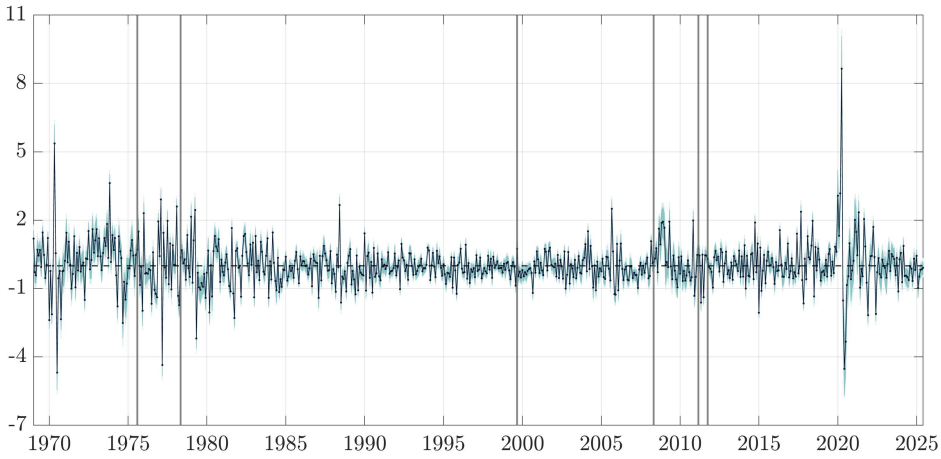

Notes: Shaded bands show 68% (inner) and 90% (outer) credible sets for monthly shocks. The solid line represents the posterior mean. Vertical bars correspond to the narrative restriction episodes.

Over a longer history, transportation shocks display medium-frequency waves—

episodes of tightness followed by easing—with positive clusters in the early–mid 1970s, around the mid-2000s, and again in 2021–2022. Distinct one-off peaks line up with well-known disruptions to ocean and air freight capacity (early 1995 Kobe, spring 2010 airspace closures, late-2016 Hanjin, spring 2021 Suez, late-2023 canal/route restrictions), consistent with the shipping cycle where slow supply adjustment interacts with demand (Stopford, 2009). Input-production shocks are more episodic, showing short bursts rather than long runs, with spikes in the mid-1970s, a clear reduction during the Great Moderation from 1990 to 2007, and again higher volatility around the GFC and with the onset of the pandemic.

3.2 Impulse response analysis

Fig. 3 displays impulse responses of all variables to a rise of one standard deviation of each of the three structural shocks. Shaded areas are robust credible regions in the sense of GKR23, with the darker band showing the 68% region and the lighter band the 90% region.

For a contractionary transportation supply shock, exhibited in the top row, transportation costs jump on impact and exhibit a hump-shape within the first year before gradually returning toward zero after about three years. Supplier delivery time rises on impact due to constraints in transportation capacity that lead to delayed shipping, then overshoot into negative territory between 18 to 30 months, before normalizing thereafter. World industrial production declines on impact, then overshoots for a few months, before turning back into negative territory around one year after the shock.

For a negative input-production supply shock, exhibited in the middle row, transportation costs drop modestly on impact decaying toward zero within two to three years. Supplier delivery time rises on impact and then converges back to zero with a temporary very moderate undershooting. World industrial production declines persistently by an economically meaningful amount, highlighting the real effects of complex global value chains with highly specified input goods.

For a positive global demand shock, shown in the bottom row, transportation costs and supplier delivery time (SDT) both increase on impact. Transportation cost build up until one year before converging back to zero after two years. SDT peaks after 6 months, converges more quickly back to zero before it undershoots for some time. World industrial production rises and remains positive over the horizon of the impulse response of 5 years. The very presistent output respose of the global demand shock is rather untypical for demand-side factors, which are usually assumed to return to zero after some time (Blanchard and Quah, 1989). We leave the long-run response of industrial production to global demand unrestricted, and our result points in the

Figure 3: Impulse responses

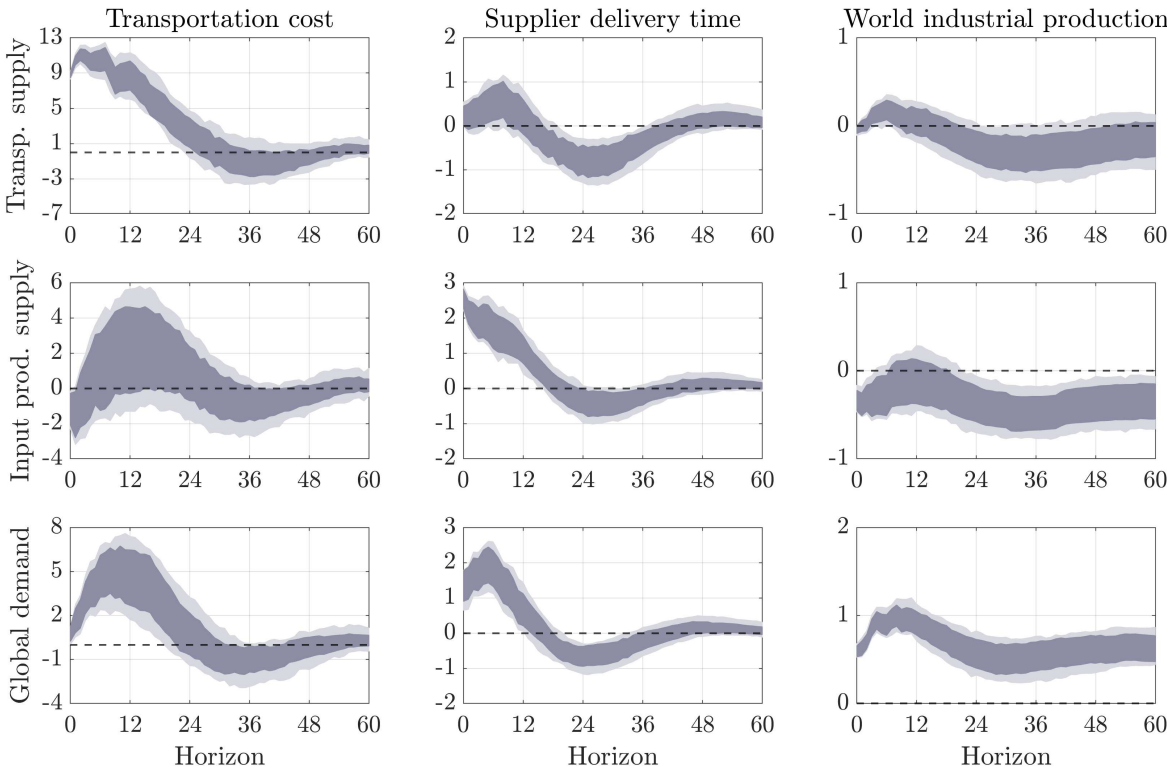

Notes: Responses to a one–standard deviation structural shock. Dark band: 68% robust credible set; light band: 90% robust credible set (Giacomini–Kitagawa–Read). Monthly horizons. Variables (columns): transportation costs, supplier delivery time, world industrial production. Shocks (rows): transportation supply, input-production supply, global demand. Restrictions combine sign, boundary, and narrative restrictions. Responses for world industrial production (shown in cumulative form) and for the transportation-cost index are read as percentage deviations from the pre-shock level, while responses for supplier delivery time are measured in index points.

direction of hysteresis effects discussed in the literature (Furlanetto et al., 2025).

3.3 Forecast error variance decomposition

Next, we turn to the forecast error variance decomposition. Fig. 4 reports the share of the forecast error variance explained by each structural shock (rows) for each observable (columns). Shaded areas are robust credible regions in the sense of GKR, with the darker band showing the 68% region and the lighter band the 90% region; horizons are monthly.

Three observations are worth mentioning. First, transportation costs are predominantly driven by the transportation supply shock at all horizons: its share is near one on impact and remains high (around 0.7–0.8) even at the horizon of five years. The global demand shock contributes modestly, rising toward roughly one-third by one year and thereafter, while the input-production shock accounts for a small and

relatively flat share (about 0.1–0.15 at longer horizons). Second, supplier delivery time are mostly determined by the input-production shock, around 0.8–0.9 on impact, with this share declining over time toward roughly 0.3 as the global demand shock takes over, gradually rising to about 0.5–0.6 within the first years after the shock impulse. The transportation supply shock explains only a limited and gradually increasing fraction of delivery-time variance (toward ∼0.2 by the end of the horizon). Third, world industrial production is dominated by the global demand shock at short horizons with a share close to one on impact; both input-production shocks account for non-negligible fractions at medium to long horizons rising toward ∼0.2 while the transportation shock plays only a minor role for industrial production.

Figure 4: Forecast error variance decomposition

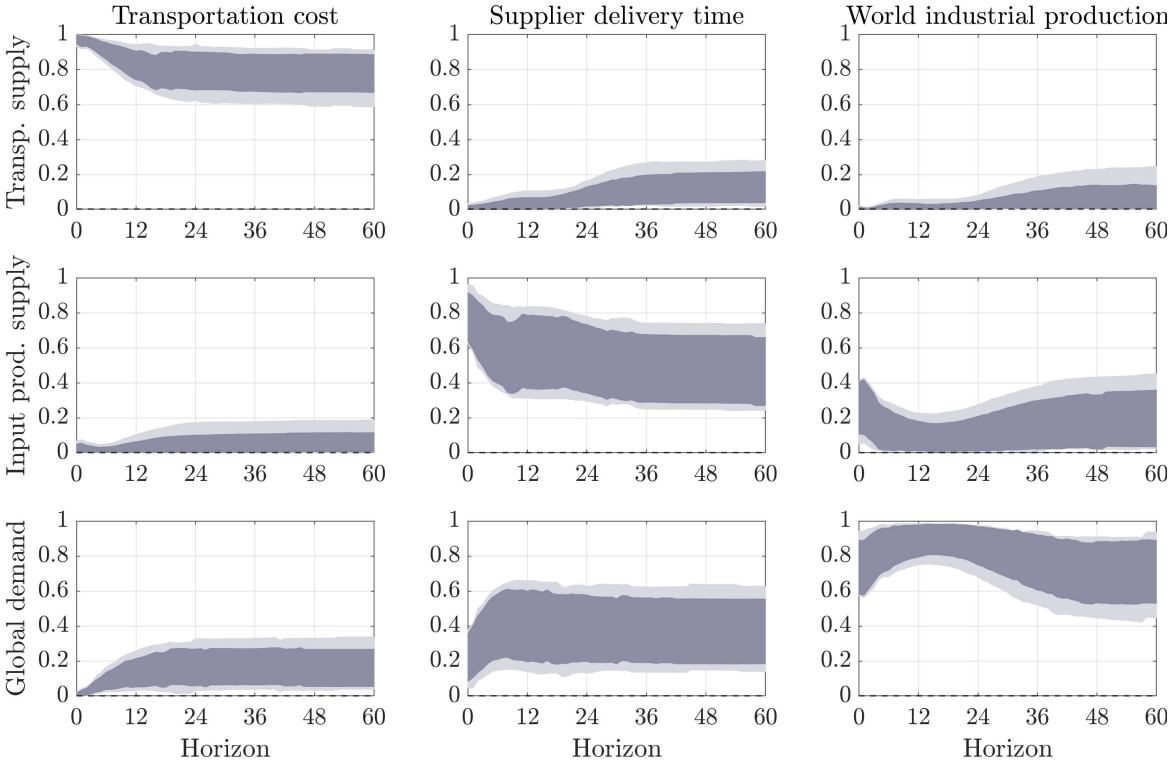

Notes: Rows are shocks (transportation supply; input-production supply; global demand). Columns are variables (transportation costs; supplier delivery time; world industrial production). Dark band: 68% robust credible set; light band: 90% robust credible set (GKR). Monthly horizons (0–60).

3.4 Measuring global sectoral supply chain tensions

We use the estimated model to construct an indicator of tensions in global supply chains from the SVAR's historical decomposition. For each month, we sum the contributions of the two sectoral supply shocks —transportation and input production

— for the two variables (i) supplier delivery time and (ii) real transportation costs. Summing the share each shock explains in the historical evolution of these two series seems to be an intuitive measure of global disruptions at the sectoral level.

Fig. 5a plots our favourite measure as solid blackline, which we label 'Global supply chain tension index' (GSTIX). The shaded area around are the credible sets, as before. As a benchmark, the chart also features the Global Supply Chain Pressure Index (GSCPI) Benigno et al. (2022). As becomes clear, the two measures co-move strongly around major episodes—including the pandemic surge—with a contemporaneous correlation of about 0.65 over the overlapping sample. During early 2020 the GSTIX spikes on impact and remains elevated through subsequent waves and reopenings; a shorter rise appears around the Shanghai lockdown in 2022m4. During the first ten years of the 2000s, our measure shows more persistence and pronounced swings in global supply chains.

The identification of two shocks along the supply chain allows us to differentiate these alternative sources of disturbances. We construct two sub-indices analogously: Global supply chain tensions due to transportation (GSTIX-T, Fig. 5b) sum over transportation-shock contributions, and global supply chain tensions related to input production sum over input-production-shock contributions (GSTIX-I, Fig. 5c). By construction, these two components add up to the GSTIX. Decomposition shows that most of the pandemic surge is attributable to transportation-supply disruptions, consistent with capacity reductions and logistics frictions documented during Covid-19 (Heiland and Ulltveit-Moe, 2020). Before the pandemic, the GSTIX displays marked cycles that align with the global shipping cycle: a peak in 2003–2004 associated with the China-led trade expansion and subsequent fleet growth (Stopford, 2008), and a peak around the 2008–2009 crisis amid the collapse in trade, fleet imbalances, and scrapping (Notteboom et al., 2021). Input-production disruptions contribute episodically, including around natural-disaster and supply-network events, consistent with the propagation of shocks through production networks (Acemoglu and Tahbaz-Salehi, 2020). Overall, the GSTIX provides a structural, model-based gauge of supply-side strain that complements the reduced-form GSCPI, while allowing a clean split between transportation and input-production sources.

Finally, we build on the third identified shock that purged our analysis on supply shocks from global aggregate demand effects and associate the share explained by the aggregate demand shock to supplier delivery time and transportation cost with the extent of congestion in supply chains, labeling it as *Global Supply Chain Congestion Index*. Fig. 6 reports the GSCIX, which isolates demand-driven tightness. The index falls steeply in global downturns (e.g., 2009; early 2020) and rises during rebounds

Figure 5: Global Supply Chain Tension Indicators

(a) Global supply chain tension index (GSTIX)

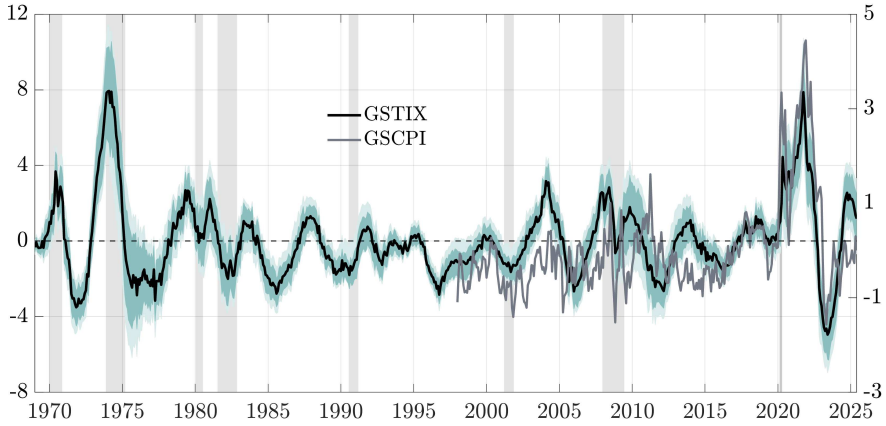

(b) Global supply chain tension index, transportation (GSTIX-T)

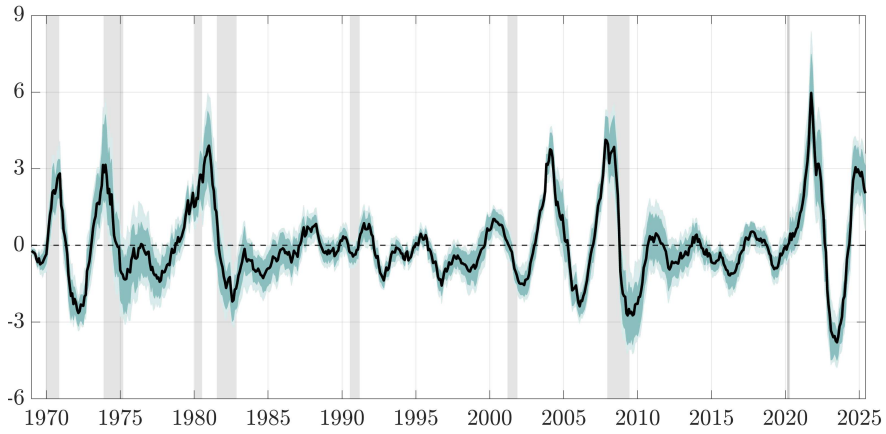

(c) Global supply chain tension index, input production (GSTIX-I)

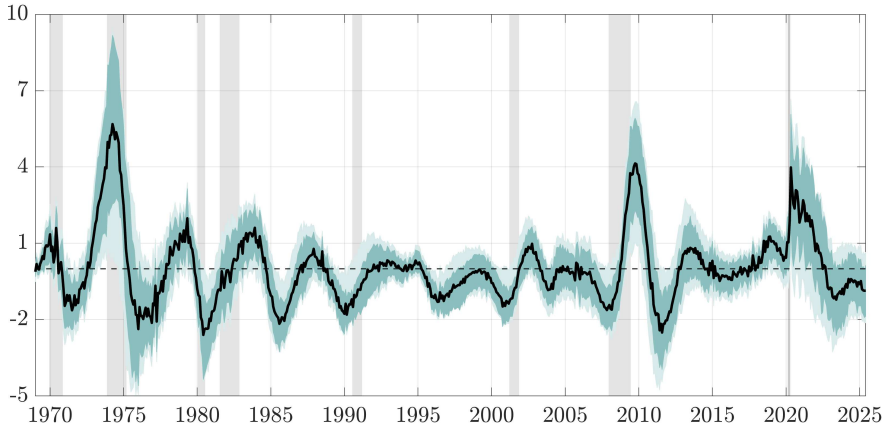

Notes: Vertical grey bars denote NBER U.S. recessions. Panel (a): Black line = GSTIX (mean); grey line (right axis) = GSCPI (Benigno et al., 2022). Panel (b): GSTIX-T is constructed as the sum of transportation-shock contributions to supplier delivery time and transportation costs; black line = mean. Panel (c): GSTIX-I is constructed as the sum of input-production-shock contributions to supplier delivery time and transportation costs; black line = mean; shaded bands = 68% and 90% robust credible sets.

(2003–2005; 2010–2011; 2021–2022), consistent with demand surges elongating delivery times and supporting freight rates even absent additional supply frictions. Relative to the supply components, the congestion index is more symmetric around zero over medium horizons.

Figure 6: Global Supply Chain Congestion Index

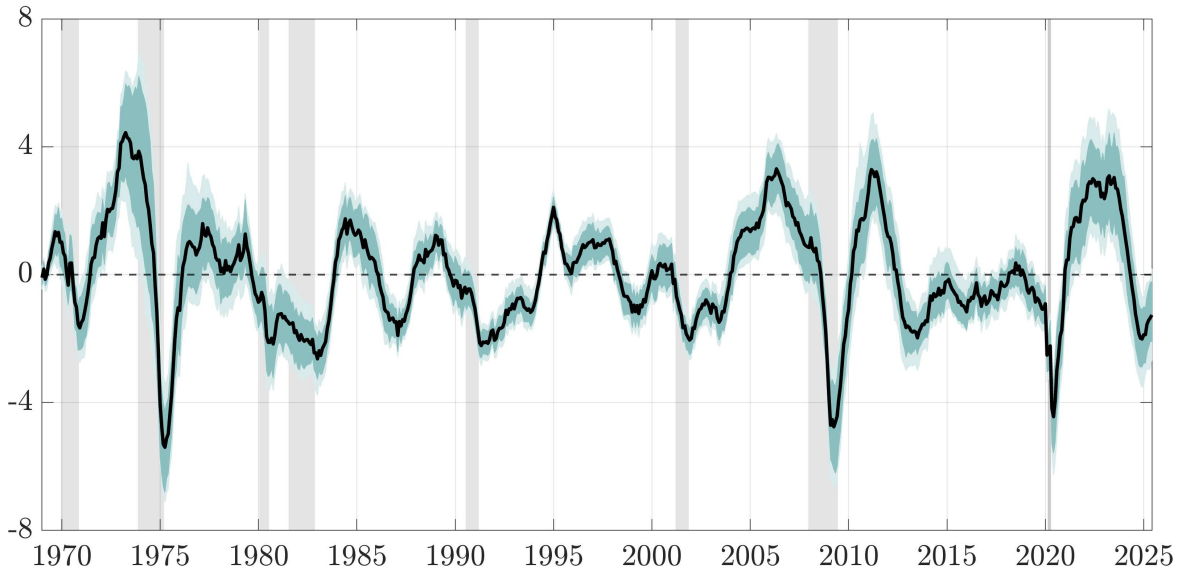

Notes: Sum of the global demand shock's contributions to supplier delivery time and transportation costs. Black line = mean; shaded bands = 68% and 90% robust credible sets. This is a demand-driven congestion measure, separate from the supply-side indices.

4 Macroeconomic effects

4.1 Robust block-exogenous VAR

We quantify spillovers using a monthly block-exogenous VAR in which the identified global sectoral shocks are predetermined with respect to all variables that enter the exogenous block (Cushman and Zha, 1997). Let Y_t collect the three baseline global variables—transportation cost s_t, supplier delivery time z_t, and world industrial production y_t—ordered as $(s_t, z_t, y_t)'$. For each block $b \in \{\text{US}, \text{COM}\}$ with block vector $X_t^{(b)}$, we estimate

$$\begin{bmatrix} Y_t \\ X_t^{(b)} \end{bmatrix} = \begin{bmatrix} \alpha \\ c^{(b)} \end{bmatrix} + \begin{bmatrix} A(L) & 0 \\ C^{(b)}(L) & D^{(b)}(L) \end{bmatrix} \begin{bmatrix} Y_t \\ X_t^{(b)} \end{bmatrix} + \begin{bmatrix} B & 0 \\ E^{(b)} & F^{(b)} \end{bmatrix} \begin{bmatrix} \varepsilon_t^Y \\ \varepsilon_t^{(b)} \end{bmatrix}, \qquad (12)$$

with $p = 12$ lags and a deterministic trend. The upper-right zero block rules out contemporaneous feedback from $X_t^{(b)}$ to Y_t, while baseline shocks ε_t^Y may load contemporaneously into $X_t^{(b)}$ via $E^{(b)}$.

The U.S. block $X_t^{(\mathrm{US})}$ includes industrial production, inventories, PCE inflation, core PCE inflation, the producer price inflation, the 1-year treasury rate, and the unemployment rate. The commodity/oil block $X_t^{(\mathrm{COM})}$ includes the real price of oil and a broad commodity price index. The two models are estimated over the sample period 1968-01 to 2025-06, see Online Appendix B.1 for a description of the data. For each accepted baseline draw, these series load contemporaneously on the identified global shocks through $b^{(\cdot)}$, allowing us to trace price pass-through conditional on the same dynamics at a global level.

All quantity and price variables enter in first differences of logs (except inventories that are in first difference of level); interest rates and unemployment rates are in levels. IRFs for differenced series are shown in cumulative form. Regarding estimation, we keep the same approach as in the baseline VAR and implement the robust Bayesian procedure of Giacomini and Kitagawa (2021) and Giacomini et al. (2023) under our sign, boundary, and narrative restrictions. We retain *1,000* accepted (ϕ, Q) draws that satisfy all restrictions. For each accepted draw, we (i) recover the baseline structural shocks ε_t^Y, (ii) estimate each block in (12) by OLS conditional on those shocks and on lags of $(Y_t, X_t^{(b)})$ (point estimate for the block), and (iii) build the implied augmented system to compute IRFs and historical decompositions. We report 68% and 90% GKR volume-optimized robust credible regions C_α^*, which are valid regardless of the choice of unrevisable prior on the flat part of the likelihood.

4.2 Dynamic response of the U.S. economy

This section quantifies how the two identified global sectoral supply shocks propagate to U.S. real activity, prices, and monetary policy within the block-exogenous VAR. Fig. 7a and Fig. 7b display impulse responses to a one–standard-deviation shock; shaded (solid) bands are 68% (90%) robust credible regions based on the accepted draws from the baseline identification. For differenced series the figures report cumulative responses.

A negative transportation supply shock is contractionary for U.S. real activity and pushes prices up, but the monetary-policy response is limited. Industrial production falls on impact by a few tenths of a percentage point, briefly recovers, and then declines again so that output remains below baseline at medium horizons, although by less than under the input-production shock. Inventories show a modest short-run accumulation followed by a prolonged drawdown, consistent with goods being delayed and then worked off once bottlenecks ease. The unemployment rate rises gradually and peaks after roughly three years, pointing to a persistent though moderate weakening of the labor market. Producer prices display a pronounced hump, with PPI peaking at

Figure 7: IRFs of transportation and input-production supply shocks on U.S. variables

(a) Transportation supply shock

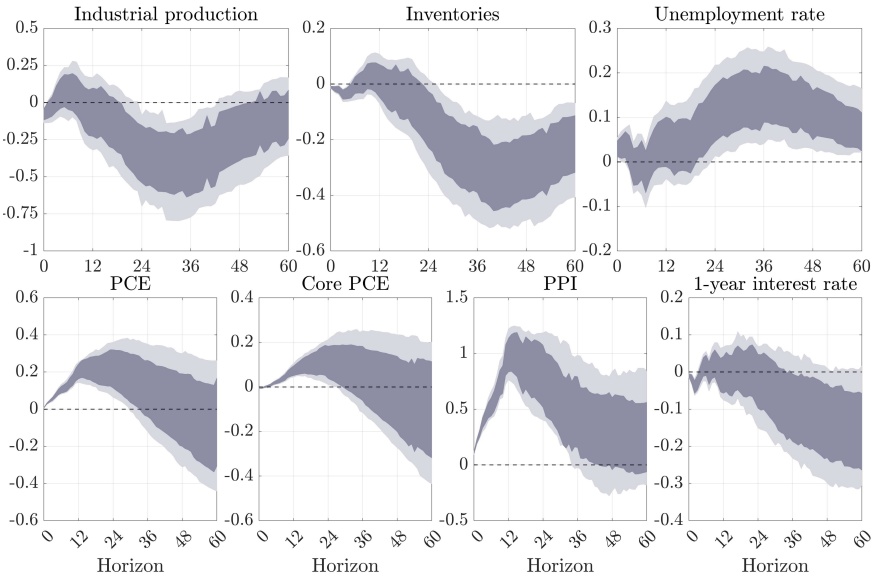

(b) Input-production supply shock

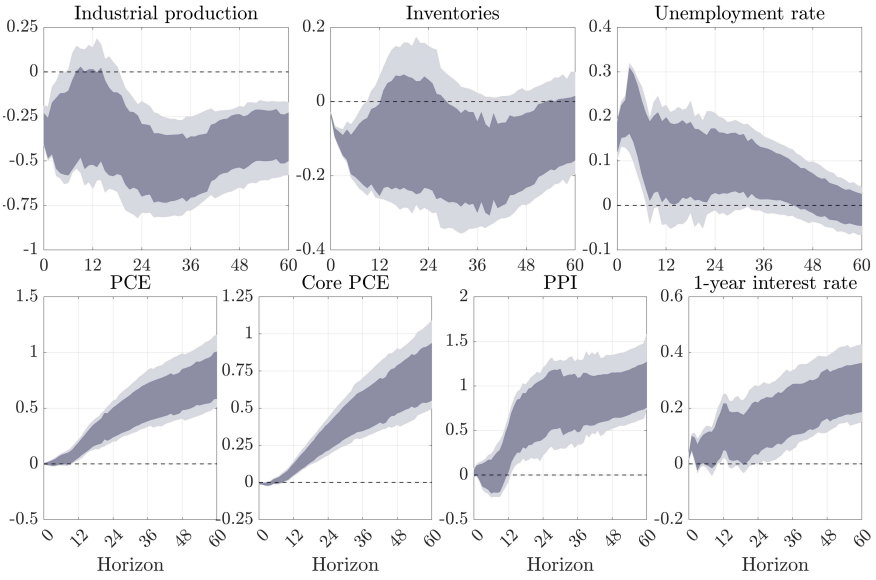

Notes: Shaded (solid) bands are 68% (90%) robust credible regions. Responses are to a one–standard-deviation shock of the indicated type. Impulse responses for industrial production, PCE and core PCE prices, the producer price index, and business inventories are shown in cumulative form and should be read as percentage deviations from the pre-shock level, whereas responses for the unemployment rate and the short-term interest rate are measured in percentage points.

around 1 percentage point after about one year before slowly retracing. The pass-through to consumer prices is more muted: the PCE and core PCE price levels drift up by only a few tenths of a percentage point and flatten after roughly two years. The one-

year interest rate moves slightly down over the horizon, indicating that monetary policy mostly looks through the temporary cost-push inflation associated with transportation tensions.

A negative input production shock generates a stronger and more persistent stagflationary pattern. Industrial production drops sharply on impact, remains persistently below baseline, and shows no clear recovery within the five-year window. Inventories decline steadily as firms run them down in response to shortages of inputs, while the unemployment rate rises more markedly and stays elevated, signaling a deeper and longer-lasting contraction than under a transportation shock. Price dynamics are also stronger: PPI increases quickly and reaches a sizeable hump that persists over several years, and both the PCE and core PCE price levels rise more and for longer than under a transportation shock, with peaks occurring toward the end of the horizon. In contrast to the transportation case, the one-year interest rate increases persistently by several tenths of a percentage point, revealing a systematic monetary tightening in response to the more durable inflationary pressures generated by input-production bottlenecks.

4.3 Commodity prices

This section summarizes how the two global sectoral supply shocks propagate to world commodity prices. The commodity block includes the *real price of oil* and a broad *commodity price index*. Figure 8a displays impulse responses to a one–standard-deviation transportation supply shock, and Figure 8b displays the corresponding responses to an input production shock.

A negative transportation supply shock raises commodity prices on impact. The real price of oil jumps in the very short run, reaches a clear peak after roughly one year, and then gradually declines toward baseline, with the credible regions overlapping zero at longer horizons. The broad commodity price index exhibits a pronounced hump-shaped response: it increases during the first year, peaks within that window, and then retraces, with effects that become small and may turn slightly negative at very long horizons. Overall, transportation shocks generate a sizable but largely temporary spike in the broad commodity basket and a more modest, uncertain medium-run effect on oil prices.

An adverse input production shock delivers a more persistent pattern. The real price of oil moves below baseline initially and remains negative for several quarters, then turns positive around the one-year mark and continues to rise, reaching a peak after about two to three years and remaining clearly above zero at the end of the horizon. The broad commodity price index increases more smoothly: it drifts upward

over the first year and stays persistently positive over the medium run, with little sign of a complete reversion. Compared with transportation shocks, input production shocks generate more sustained medium-run increases in both oil and the broader commodity index, consistent with more durable upstream cost pressures.

Figure 8: IRFs of transportation and input-production supply shocks in the commodity block

(a) Transportation supply shock

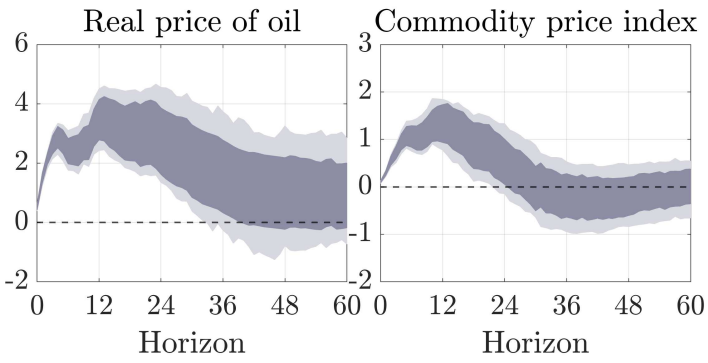

(b) Input-production supply shock

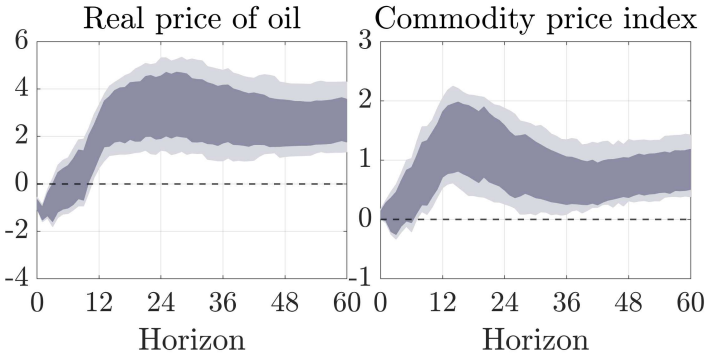

Notes: Shaded bands are 68% for the darker and 90% for the lighter robust credible regions. Responses are to a one–standard-deviation shock of the indicated type. Impulse responses for the real price of oil and for the broad commodity price index are shown in cumulative form and should be read as percentage deviations from the pre-shock level.

4.4 Post-pandemic inflation

Tab. 3 reports annual historical-decomposition contributions of the two global sectoral supply shocks to post-pandemic inflation outcomes in the United States over 2022–2024. The reported values are obtained from the historical decompositions of the block-exogenous VAR and measure the cumulative contribution of each identified shock to year-over-year consumer and producer price inflation. We focus here on the behavior

of U.S. in the immediate post-pandemic period. Online Appendix D.1 documents the full set of historical decompositions over the entire sample.

In 2022, both transportation and input-production shocks pushed up consumer prices, as shown by positive contributions to PCE and core PCE, with input-production playing at least as important a role as transportation. The inflation impulse is even stronger in producer prices: PPI records large positive contributions, with input-production shocks accounting for the bulk of the increase. In 2023, transportation shocks reverse and exert a disinflationary influence on PCE and PPI, while input-production shocks continue to add modestly to PCE and core PCE and provide at most a small positive contribution to PPI. By 2024, the contributions of both shocks to consumer prices are small and often not statistically different from zero, whereas transportation shocks again provide a clearly positive contribution to PPI, consistent with lingering cost pressures upstream even as headline and core inflation normalize.

Table 3: Post-pandemic contributions

	2022		**2023**		**2024**	
Series	**Transp.**	**Input**	**Transp.**	**Input**	**Transp.**	**Input**
United States						
PCE	4.62		2.05		2.09	
	[0.53, 2.06]	[0.88, 4.51]	[-1.66, -0.12]	[0.38, 4.03]	[-0.48, 0.94]	[-0.07, 3.63]
Core PCE	4.00		2.29		2.25	
	[0.62, 2.06]	[0.97, 4.55]	[-0.99, 0.41]	[0.60, 4.31]	[-0.81, 0.57]	[-0.03, 3.68]
PPI	6.27		-3.40		1.30	
	[-1.50, 2.02]	[2.97, 6.49]	[-7.73, -4.03]	[-0.70, 3.24]	[2.96, 5.62]	[-0.14, 3.76]

Notes: Entries are annual historical-decomposition contributions to year-over-year rates, in percentage points. Columns are years × shocks; for each series, the first row is the demeaned series value spanning all shocks per year, and the second row lists the 68% robust credible region for each shock's contribution, shown in square brackets.

These post-pandemic patterns are in line with the dynamic propagation as reported in the impulse responses. Transportation bottlenecks account for much of the 2022 run-up in consumer and especially producer prices, while input-production shortages generate more persistent contributions, particularly to producer-price inflation. As tensions in supply chains fade during 2023, transportation contributions shrink or turn negative; by 2024, sectoral-supply effects on consumer inflation are small and the remaining influence of these shocks is concentrated upstream in producer prices. This interpretation is consistent with evidence on capacity constraints and port congestion during 2021–2022 (Comin et al., 2023; Bai et al., 2024), and with concurrent roles for labor-market tightness and demand rebalancing (Benigno and Eggertsson, 2023; Fornaro and Romei, 2022). Our estimates for supply-side contributions are below those of other studies that incorporate supply-chain indicators (Ferrante et al., 2023;

di Giovanni et al., 2022).

5 Conclusion

We propose a structural vector autoregressive (SVAR) model to identify two global sectoral supply shocks: a transportation supply shock and an input-production supply shock. Augmenting the model by global demand disturbances, we are able to trace tensions in global supply chains from three distinct sources: supply-tensions arising in the transportation sector, supply-tensions arising from intermediate input production, and demand-induced congestion effects. We build indices at monthly frequency from 1969 to 2024 that allow to track the evolution and dynamic implications over time, by summing over the historical contribution of each shock to supplier delivery time and real transportation costs.

We interpret the resulting shocks as global and explore the dynamic propagation to the U.S. economy and commodity markets. The shocks pass through to prices and monetary policy in a systematic, but shock-specific, way. Transportation shocks generate a moderate and relatively short-lived increase in consumer prices, with a pronounced but temporary hump in producer prices and little evidence of systematic tightening in the one-year interest rate, consistent with monetary policy largely looking through a transitory cost-push episode. Input-production shocks, by contrast, induce a deeper and more persistent decline in industrial production, a larger and longer-lasting rise in PPI, and more sustained increases in PCE and core PCE, to which monetary policy responds with a clear and persistent tightening.

The model also provides new insights for the post-pandemic inflation surge. In 2022, both sectoral shocks contributed positively to U.S. consumer prices, with particularly large contributions to producer prices from input-production shocks. In 2023, transportation shocks became disinflationary, as congestion eased, while input-production shocks still added modestly to inflation. By 2024, the contributions of both shocks to consumer inflation were small and often indistinguishable from zero, with the remaining influence of sectoral supply shocks concentrated upstream in producer prices.

Overall, the evidence highlights that distinguishing transportation from input-production tensions is an important differentiation for understanding global supply chain bottlenecks and the resulting dynamic real and nominal effects. The developed indices should provide useful information for policymakers to design adequate stabilization policies.

References

Acemoglu, D., Carvalho, V., Ozdaglar, A., and Tahbaz-Salehi, A. (2012). The network origins of aggregate fluctuations. *Econometrica*, 80(5):1977–2016.

Acemoglu, D. and Tahbaz-Salehi, A. (2020). Firms, failures, and fluctuations: The macroeconomics of supply chain disruptions. NBER Working Paper 27565.

Afrouzi, H. and Saroj, B. (2023). Inflation and GDP dynamics in production networks: A sufficient statistics approach. NBER Working Paper 31218.

Alessandria, G., Khan, S. Y., Khederlarian, A., Mix, C., and Rhul, K. J. (2023). The aggregate effects of global and local supply chain disruptions: 2020-2022. *Journal of International Economics*, 146:103788.

Arias, J. E., Rubio-Ramirez, J. F., and Waggoner, D. F. (2018). Inference based on structural vector autoregressions identified with sign and zero restrictions: Theory and applications. *Econometrica*, 86(2):685–720.

Bai, X., Fernandez-Villaverde, J., Li, Y., and Zanetti, F. (2024). The causal effects of global supply chain disruptions on macroeconomic outcomes: Evidence and theory. NBER Working Paper 32098.

Baqaee, D. R. (2018). Cascading failures in production networks. *Econometrica*, 86(5):1819–1838.

Barrot, J.-N. and Sauvagnat, J. (2016). Input specificity and the progagation of idiosyncratic shocks in production networks. *Quarterly Journal of Economics*, 131(3):1543–1592.

Baumeister, C. and Hamilton, J. (2019). Structural interpretation of vector autoregressions with incomplete identification: Revisiting the role of oil supply and demand shocks. *American Economic Review*, 109(5):1873–1910.

Baumeister, C. and Hamilton, J. D. (2015). Sign restrictions, structural vector autoregressions, and useful prior information. *Econometrica*, 83(5):1963–1999.

Benigno, G., di Giovanni, J., Groen, J. J., and Noble, A. I. (2022). The GSCPI: A new barometer of global supply chain pressures. Federal Reserve Bank of New York Staff Papers 1017.

Benigno, P. and Eggertsson, G. B. (2023). It's baaack: The surge in inflation in the 2020s and the return of the non-linear Phillips curve. NBER Working Paper 31197.

Besedeša, T. and Murshid, A. P. (2018). Experimenting with ash: The trade-effects of airspace closures in the aftermath of Eyjafjallajökull. FREIT Working Paper 1397.

Blanchard, O. and Quah, D. (1989). The dynamic effects of aggregate demand and supply disturbances. *American Economic Review*, 79(4):655–673.

Boehm, C. E., Flaaen, A., and Pandalai-Nayar, N. (2019). Input linkages and the transmission of shocks: Firm-level evidence from the 2011 Tōhoku earthquake. *Review of Economics and Statistics*, 101(1):60–75.

Budd, L., Griggs, S., Howarth, D., and Ison, S. (2010). A fiasco of volcanic proportions? Eyjafjallajökull and the closure of European airspace. *Mobilities*, 6(1):31–40.

Bureau of Transportation Statistics (2021). Suez canal blockage by Ever Given will affect U.S. ports, businesses, consumers. Data spotlight.

Burriel, P., Kataryniuk, I., Monero Pérez, C., and Viani, F. (2024). A new supply bottleneck index based on newspaper data. *International Journal of Central Banking*, 20(2):17–67.

Caldara, D., Iacoviello, M., and Yu, D. (2025). Measuring shortages since 1900. International Finance Discussion Paper 1407.

Cannella, S., Dominguez, R., Ponte, B., and Framinan, J. M. (2018). Capacity restrictions and supply chain performance: Modelling and analysing load-dependent lead times. *International Journal of Production Economics*, 204:264–277.

Carvalho, V., Nirei, M., Saito, Y., and Tahbaz-Salehi, A. (2021). Supply chain disruptions: Evidence from the Great East Japan earthquake. *The Quarterly Journal of Economics*, 136(2):1255–1321.

Chang, S. E. (2000). Disasters and transportation systems: Loss, recovery and competition at the port of Kobe after the 1995 earthquake. *Journal of Transport Geography*, 8(1):53–65.

Chico, C., Wang, Z., Reyes, E. K. C., and Mariasingham, M. J. (2024). Ais-based framework for analyzing the impacts of passageway disruptions. *Economics of Disasters and Climate Change*, 8:489–511.

Coşar, A. K., Osotimehin, S., and Popov, L. (2024). The long-run effects of transportation productivity on the US economy. NBER working paper 33248.

Comin, D. A., Johnson, R. C., and Jones, C. J. (2023). Supply chain constraints and inflation. NBER Working Paper 31179.

Cushman, D. O. and Zha, T. (1997). Identifying monetary policy in a small open economy under flexible exchange rates. *Journal of Monetary Economics*, 39(3):433–448.

Daudin, G., Héricourt, J., and Patureau, L. (2022). International transportation costs: New findings from modeling additive cost. *Journal of Economic Geography*, 22(5):989–1044.

Dew-Becker, I. (2023). Tail risk in production networks. *Econometrica*, 91(6):2089–2123.

Dhyne, E., Kikkawa, A., Mogstad, M., and Tintelnot, F. (2021). Trade and domestic production networks. *Review of Economic Studies*, 88(2):643–668.

di Giovanni, J., Kalemli-Özcan, S., Silva, A., and Yildirim, M. A. (2022). Global supply chain pressures, international trade, and inflation. NBER Working Paper 30240.

Ferrante, F., Graves, S., and Iacoviello, M. (2023). The inflationary effects of sectoral reallocation. *Journal of Monetary Economics*, 140(Supplement):S64–S81.

Fornaro, L. and Romei, F. (2022). Monetary policy during unbalanced global recoveries. CEPR Discussion Paper DP16971.

Forslid, R. and Sanctuary, M. (2023). Climate risks and global value chains: The impact of the 2011 Thailand flood on swedish firms. CEPR Discussion Paper DP17855.

Friedt, F. L. (2021). Natural disasters, aggregate trade resilience, and local disruptions: Evidence from Hurricane Katrina. *Review of International Economics*, 29(5):1081–1120.

Frittelli, J. (2005). Hurricane Katrina: Shipping disruptions. Crs report for congress.

Furlanetto, F., Lepetit, A., Robstad, Ø., Rubio-Ramírez, J., and Ulvedal, P. (2025). Estimating hysteresis effects. *American Economic Journal: Macroeconomics*, 17(1):35–70.

Giacomini, R. and Kitagawa, T. (2021). Robust Bayesian inference for set-identifed models. *Econometrica*, 89(4):1519–1556.

Giacomini, R., Kitagawa, T., and Read, M. (2023). Identification and inference under narrative restrictions. Research Discussion Paper RDP 2023-07, Reserve Bank of Australia.

Guerrieri, V., Lorenzoni, G., Straub, L., and Werning, I. (2022). Macroeconomic implications of COVID-19: Can negative supply shocks cause demand shortages? *American Economic Review*, 112(5):1437–1474.

Gulley, A. L. (2022). One hundred years of cobalt production in the Democratic Republic of the Congo. *Resources Policy*, 79:103007.

Habib, K., Hamelin, L., and Wenzel, H. (2016). A dynamic perspective of the geopolitical supply risk of metals. *Journal of Cleaner Production*, 133:850–858.

Haraguchi, M. and Lall, U. (2015). Flood risks and impacts: A case study of Thailand's floods in 2011 and research questions for supply chain decision making. *International Journal of Disaster Risk Reduction*, 14:256–272.

Heiland, I. and Ulltveit-Moe, K. (2020). An unintended crisis in sea transportation due to COVID-19 restrictions. In Baldwin, R. and Evenett, S. J., editors, *COVID-19 and Trade Policy: Why Turning Inward Won't Work*. CEPR Press.

Hiroshi, F. and Hsiao, C. (2015). Disentangling the effects of multiple treatments—measuring the net economic impact of the 1995 Great Hanshin-Awaji earthquake. *Journal of Econometrics*, 186(1):66–73.

Horvath, M. (2000). Sectoral shocks and aggregate fluctuations. *Journal of Monetary Economics*, 45(1):69–106.

Huang, R., Malik, A., Lenzen, M., Jin, Y., Wang, Y., Faturay, F., and Zhu, Z. (2022). Supply-chain impact of Sichuan earthquake: A case study using disaster input-output analysis. *Natural Hazards*, 2022(110):2227–2248.

Hummels, D., Lugovskyy, V., and Skiba, A. (2009). The trade reducing effects of market power in international shipping. *Journal of Development Economics*, 89(1):84–97.

Hummels, D. and Skiba, A. (2004). Shipping the good apples out? Confirmation of the Alchian-Allen conjecture. *Journal of Political Economy*, 112(6):1384–1402.

ITF (2024). The Red Sea crisis: Impacts on global shipping and the case for international co-operation. Background paper, International Transport Forum, OECD.

Känzig, D. and Raghavan, R. (2025). The macroeconomic effects of supply chain shocks: Evidence from global shipping disruptions. mimeo.

Kilian, L. (2009). Not all oil price shocks are alike: Disentangling demand and supply shocks in the crude oil market. *American Economic Review*, 99(3):1053–1069.

Kilian, L. and Lütkepohl, H. (2017). *Structural vector autoregressive analysis*. Cambridge University Press.

Kilian, L. and Murphy, D. P. (2012). Why agnostic sign restrictions are not enough: Understanding the dynamics of oil market VAR models. *Journal of the European Economic Association*, 10(5):1166–1188.

Kilian, L., Nomikos, N., and Zhou, X. (2023). Container trade and the U.S. recovery. *International Journal of Central Banking*, (March 2023):417–450.

Kwon, C. (2021). Supply chain disruptions and causal outcomes: Evidence from the bankruptcy of Hanjin Shipping. working paper 3293272, SSRN.

Little, J. (1961). A proof of the queuing formula $L = \lambda W$. *Operations Research*, 3(9):383–387.

Long, J. B. J. and Plosser, C. I. (1983). Real business cycles. *Journal of Political Economy*, 91(1):39–69.

Long, J. B. J. and Plosser, C. I. (1987). Sectoral vs. aggregate shocks in the business cycle. *American Economic Review*, 77(2):39–69.

Notteboom, T., Pallis, T., and Rodrigue, J.-P. (2021). Disruptions and resilience in global container shipping and ports: The COVID-19 pandemic versus the 2008-2009 financial crisis. *Maritime Economics & Logistics*, 2021(23):179–210.

Noy, I. and duPont, W. (2016). The long-term consequences of natural disasters: Evidence from the 1999 Chi-Chi earthquake. *Economics of Disasters and Climate Change*, 1(1):21–47.

Oum, T. H., Waters, W., and Yong, J. S. (1990). A survey of recent estimates of price elasticities of demand for transport. Policy Research Working Paper Series 359, The World Bank.

Rubio-Ramírez, J. F., Waggoner, D. F., and Zha, T. (2010). Structural vector autoregressions: Theory of identification an algorithm for inference. *Review of Economic Studies*, 77:665–696.

Stopford, M. (2008). The great shipping boom 2003-8: Can we avoid a great shipping slump? Fifth City Biennial Meeting, 18-19 November 2008.

Stopford, M. (2009). *Maritime Economics*. Routledge Books, 3rd edition edition.

Suez Canal Authority (2021). Report on the grounding of MV *Ever Given*, 23–29 march 2021. Technical report, SCA.

Sytsma, T. (2020). The impact of hurricanes on trade and welfare: Evidence from US port-level exports. *Economics of Disasters and Climate Change*, 4(3):625–655.

Tjandra, S., Kraus, S., Ishmam, S., Grube, T., Linßen, J., May, J., and Stolten, D. (2024). Model-based analysis of future global tranport demand. *Transportation Research Interdisciplinary Perspective*, 23:101016.

UNISDR (2012). Annual report on disaster risk reduction 2012. Technical report, United Nations Office for Disaster Risk Reduction.